



Universiteit  
Leiden  
The Netherlands

## Transient complexes of haem proteins

Volkov, O.M.

### Citation

Volkov, O. M. (2007, February 28). *Transient complexes of haem proteins*. Leiden Institute of Chemistry/MetProt Group, Faculty of Mathematics and Natural Sciences, Leiden University. Retrieved from <https://hdl.handle.net/1887/11002>

Version: Corrected Publisher's Version

License: [Licence agreement concerning inclusion of doctoral thesis in the Institutional Repository of the University of Leiden](#)

Downloaded from: <https://hdl.handle.net/1887/11002>

**Note:** To cite this publication please use the final published version (if applicable).

## *Chapter IV*

*Dynamics in the complex  
of yeast cytochrome c and  
cytochrome c peroxidase*

## ***Abstract***

Using site-specific spin-labelling in combination with NMR spectroscopy, we have solved the solution structure of the Cyt *c* – CcP complex (Chapter III). As this transient complex is dynamic, the solution structure represents the dominant protein – protein orientation, which according to our estimates is occupied for > 70 % of the lifetime of the complex, with the rest of the time spent in the dynamic encounter state. Based on the observed paramagnetic effects, we have delineated the conformational space sampled by the protein molecules during the dynamic part of the interaction, providing experimental support for the theoretical predictions of the classical Brownian dynamics study<sup>26</sup>. Our findings corroborate the dynamic behaviour of this complex and offer an insight into the mechanism of the protein complex formation in solution.

The results presented in this chapter have been published in part as:

Volkov, A. N., Worrall, J. A. R., Holtzmann, E. & Ubbink, M. Solution structure and dynamics of the complex between cytochrome *c* and cytochrome *c* peroxidase determined by paramagnetic NMR. *Proc. Natl. Acad. Sci. U. S. A.* **103**, 18945-18950 (2006).

## ***Introduction***

A likely general feature of the macromolecular interactions, dynamics within protein complexes greatly accelerates the search of the optimal binding geometry (Chapter I). Protein mobility is particularly prominent in transient ET complexes, where fast molecular association is essential for maintaining high turn-over rates. Formation of such protein complexes can be described by a two-step model, in which a dynamic encounter state precedes a dominant, well-defined complex (Figure 1.1, p. 11). While some transient complexes exist predominantly in a single, well-defined form, others spend most of the time in the encounter state where they sample multiple protein – protein orientations (Chapter I).

It is believed that the transient ET complex of Cyt *c* and CcP exists in a single configuration for a great part of its lifetime. This is evidenced by the large NMR chemical shift perturbations (ref. 129 and Chapter V) and the fact that the crystal<sup>107</sup> and solution (Chapter III) structures of the dominant form of this complex could be solved.

However, the Cyt *c* – CcP complex is not static. Pioneering studies by FRET<sup>122,196</sup> and protein cross-linking in combination with NMR spectroscopy<sup>121</sup> have revealed the presence of multiple, quasi-isoenergetic protein – protein orientations that could undergo a dynamic interconversion within this complex in solution<sup>120</sup>. Then followed the NMR studies using hydrogen-deuterium exchange<sup>123,124</sup>, lysine modification<sup>125</sup>, and chemical shift perturbation mapping<sup>129</sup> that showed the binding surface of Cyt *c* in the complex with CcP to be broader than that suggested by the crystal or the solution structure. Moreover, in each case the binding effects at the back of Cyt *c* were observed<sup>123-125,129</sup>, implying a degree of structural rearrangement within the complex. Finally, X-ray diffraction studies of the Cyt *c* – CcP complex have revealed that CcP is well-defined in the crystals, while Cyt *c* is either completely disordered<sup>197</sup> or has large anisotropic B-factors<sup>198</sup>. Although in both cases co-crystallization artefacts cannot be entirely excluded, these observations suggest that Cyt *c* explores multiple binding sites on CcP. Based on the findings of these and other studies (for reviews see ref. 106 and 87), it has been suggested that in the initially-formed encounter complex of Cyt *c* and CcP the proteins explore a multitude of binding geometries in search of the optimal orientation for the ET<sup>120</sup>.

Despite the conclusive evidence for dynamics, the characterization of the binding interface in the encounter complex has so far proven to be elusive. Structural characterization of protein complexes using X-ray crystallography or conventional NMR spectroscopy addresses only a single, most dominant form, and till now the only way to visualize the dynamic state was offered by theoretical modelling<sup>26,27</sup>. Original Brownian dynamics simulations of the Cyt *c* – CcP complex have identified a narrow, positively-charged, lysine-rich patch on the surface of Cyt *c* that is available for the interaction with multiple binding sites provided by a broad, negatively-charged region on CcP<sup>26</sup>. Numerous attempts purporting to test this theoretical model and pinpoint the exact location of the hypothetical binding sites using site-directed mutagenesis have so far proven to be inconclusive (ref. 87 and references therein).

A unique experimental approach to visualize the dynamics within protein complexes is offered by the recent studies of non-specific protein-DNA association<sup>173,199</sup>. In an elegant work, Clore and co-workers have used intermolecular PREs and NMR spectroscopy to detect and characterise transient intermediates in protein-DNA interactions<sup>173,199</sup>. In this report we employ similar strategy to define the conformational space sampled by Cyt *c* and CcP in the dynamic encounter complex. In addition, we provide an estimate for the fraction of the lifetime of the complex spent by the proteins in the dynamic state.

By providing structural information on the dominant, well-defined form of the Cyt *c* – CcP complex (Chapter III) and its dynamic encounter state (this Chapter), this experimental approach allows us to investigate simultaneously both aspects of the complex formation in solution; therefore, it is perfectly suited for a comprehensive study of this mostly single-orientation, yet dynamic complex.

## **Results**

### ***Additional paramagnetic effects***

We have attached MTSL spin-label to different positions on the surface of CcP and observed MTSL-induced PREs of the Cyt *c* backbone amides, which were converted

into distance restraints used to calculate the structure of Cyt *c* – CcP complex in solution (Chapter III). Analysis of the solution structure shows that most of the restraints are satisfied (Figure 4.1 and Table C2 in Appendix C). The Cyt *c* residues that show distance violations, some of which as big as 10 – 15 Å, are non-randomly distributed. For instance, MTSL attached to N38C CcP exerts paramagnetic effects that map on the back of Cyt *c* (Figure 4.1 A), while MTSL at N200C CcP strongly affects the N-terminal helix (Figure 4.1 B). However, in the solution structure these residues are located too far away from MTSL. As discussed below, these additional paramagnetic effects arise from multiple Cyt *c* – CcP orientations assumed in the dynamic encounter complex.

In principle, non-specific protein interactions or Cyt *c* – CcP complexes of higher stoichiometry could contribute to the additional paramagnetic effects, which in this case would show a non-uniform concentration-dependence (see Discussion). To check for this, we have performed control experiments for N200C CcP with Cyt *c* concentration lowered five-fold (Materials and Methods). Despite the fraction of Cyt *c* available for the weaker interactions decreases from 0.10 for the samples with 1 :1 protein ratio to 0.015 in the control sample, the observed pattern of the paramagnetic effects does not change: the largest deviation of the restraint target distance is  $\pm 2$  Å for several residues (Figure 3.6 F, p. 55). Therefore, the additional paramagnetic effects are independent of the Cyt *c* concentration in the range used.

### ***Dynamic encounter complex***

We have made an estimate for the lower limit of the fraction of time spent by the proteins in the dominant orientation ( $f_{\text{dom}}$ ), based on the assumption that the paramagnetic effects for all residues with satisfied restraints arise mostly from the dominant orientation. In order to obtain the actual PREs ( $R_2^{\text{para}}$ ) for these residues, the observed PREs ( $R_{2,\text{obs}}^{\text{para}}$ ) must be multiplied by  $1/f_{\text{dom}}$  (Equation 4.1 in Materials and Methods). Protein docking performed with the  $R_2^{\text{para}}$  values corresponding to  $f_{\text{dom}} \leq 0.7$  leads to an energy increase for all solutions due to augmented van der Waals and restraint violations. In order to satisfy the shorter distance restraints resulting from low  $f_{\text{dom}}$  values, Cyt *c* should come unrealistically close to MTSL and, accordingly, CcP atoms, producing sterically-forbidden solutions.

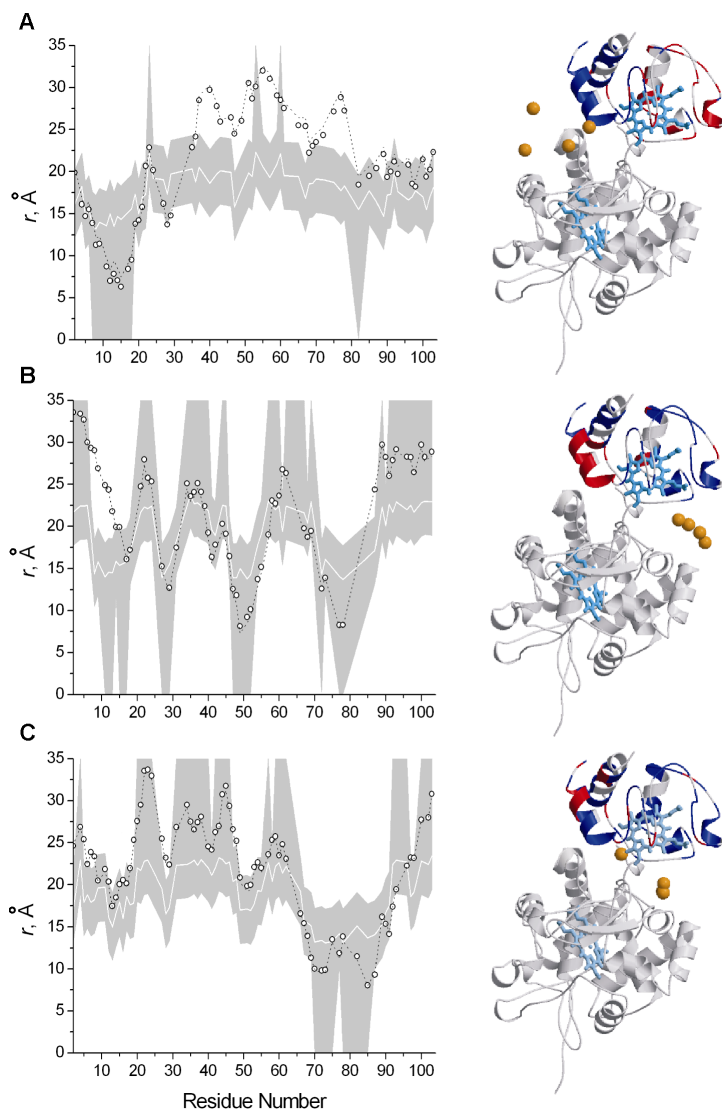


**Figure 4.1. Violation analysis of the best solution structure for the Cyt *c* – CcP complex.** The graphs illustrate the distances from the Cyt *c* backbone amide protons in the best solution structure (open circles) and crystal structure (broken line) to the averaged position of the oxygen atom of MTSL attached to CcP at N38C (A), N200C (B), and T288C (C). The white line and the shaded area indicate the PRE-derived distances and error margins, respectively, used in the structure calculations. On the right are cartoon representations of the best solution structure, indicating the residues with satisfied (blue) and violated (red) restraints. Haem groups for both proteins are in cyan. For each of the MTSL positions, four oxygen atoms, representing the conformational freedom of the spin-label, are shown as orange spheres. These were used for ensemble averaging in the structure calculations (Materials and Methods in Chapter III).

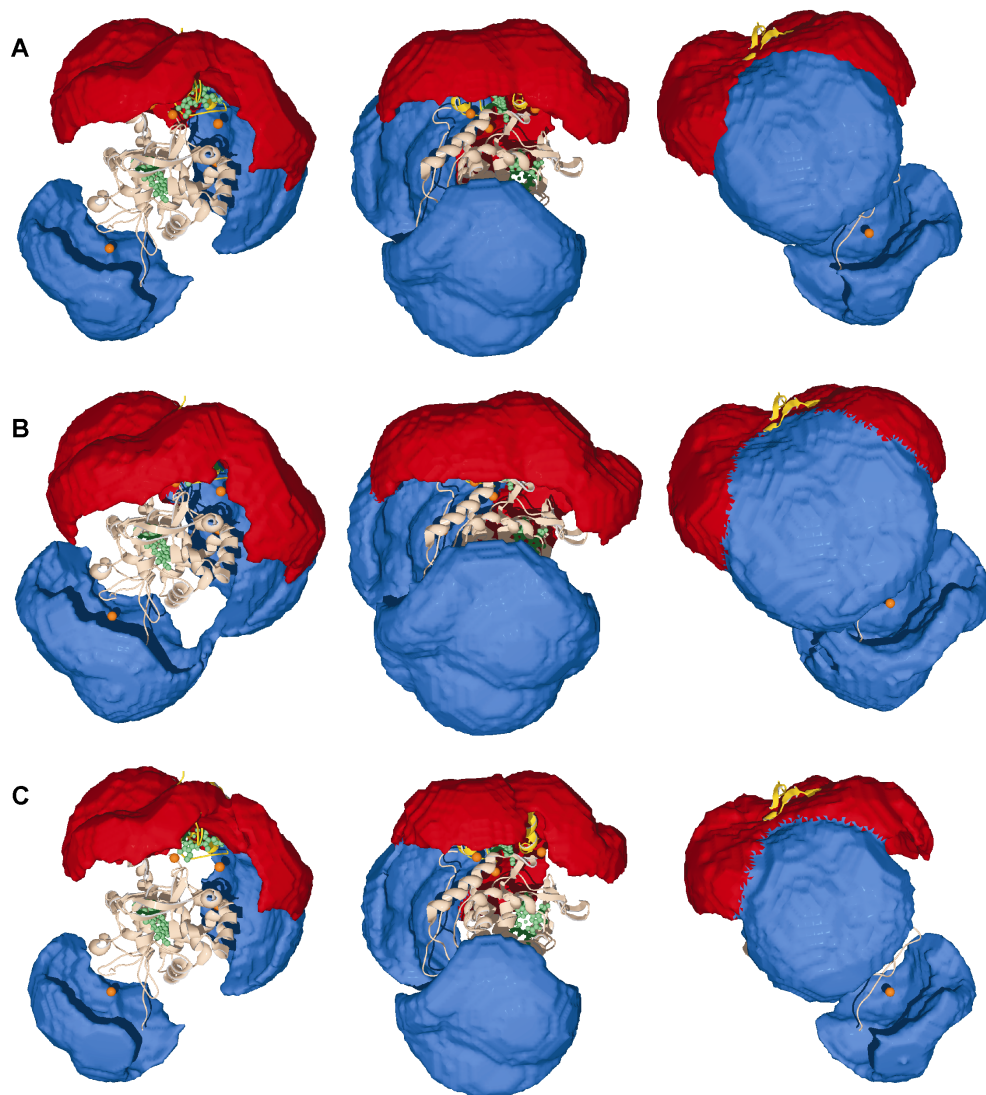


**Figure 4.2. Conformational space occupied in the Cyt *c* – CcP encounter complex.** The best solution structure is shown, rotated counter-clockwise by 120° around the vertical axis (from left to right). The orientation of the complex on the left is identical to that in Figure 4.1. CcP and Cyt *c* are shown in off-white and yellow ribbons, respectively, with haem groups in green and MTSL positions indicated by orange spheres. The red surface defines the area that must contain the centre of mass of Cyt *c* for at least 3 % (A), 10 % (B), and 1% (C) of the lifetime of the complex (outer perimeter of the red area) or less (moving from the periphery toward MTSL). The blue surface corresponds to the area that cannot be occupied by the Cyt *c* centre of mass for longer than 3 % (A), 10 % (B), and 1% (C) of the lifetime of the complex (outer perimeter of the blue area) or less (moving to the centre toward MTSL).

From this, we conclude that the proteins spend more than 70 % of the lifetime of the complex in the dominant orientation. It is impossible to identify the orientations constituting the dynamic encounter state without knowing how many of these comprise the ensemble and what fraction of the lifetime of the complex is spent in each of them (Materials and Methods). However, we can define the conformational space occupied by Cyt *c* in the encounter complex (Figure 4.2). This is achieved by mapping out the areas around those spin-labels that give rise to additional PREs (N38C, N200C, and T288C) and those that do not affect Cyt *c* atoms at all (S263C and T137C). In the dynamic state, Cyt *c* must come close to the spin-labels that cause additional PREs (the extent of approach indicated by the red area in Figure 4.2) and be far from those showing no effects (the areas to be avoided are coloured blue in Figure 4.2). The remaining space around CcP could also harbour Cyt *c* molecules; however, those would not contribute to the observed paramagnetic effects. The sizes of the areas in Figure 4.2 A correspond to a somewhat arbitrary time fraction of 3 % of the total time spent by Cyt *c* in the complex. The use of this value is justified as other fractions in the range of 1 - 30 % give rise to similar areas, which have shrunk or expanded only a little compared to that based on 3 % (Figure 4.2 B and C).

## ***Discussion***

### ***Additional paramagnetic effects***

Experimental intermolecular restraints for some of the Cyt *c* residues are violated in the lowest-energy solution structure of the Cyt *c* – CcP complex (Figure 4.1). As most of the violations are large (5 – 15 Å), they cannot be explained by small uncertainties of the backbone atom positions in the solution structure (backbone rmsd variation  $\leq 0.7$  Å, Figure 3.9 A, p. 57). Multiple rigid-body molecular dynamics runs starting from random protein positions have consistently produced a single cluster of solutions (Chapter III, Figure 3.9, p. 57), and no alternative structures that satisfy the violated restraints have been found. Attempts to compute up to three additional protein – protein orientations that, when combined with the lowest-energy solution, would satisfy all experimental restraints have

failed (data not shown), suggesting that the observed paramagnetic effects could only be explained by the combination of more than four different structures of the complex.

The observed violations cannot be accounted for by the experimental and computational errors in the calculated distance restraints as these are well within the 4 Å restraint bounds (Chapter III). To take into account yet another negative contribution to the quality of the restraints, the mobility of MTSL covalently attached to the surface of CcP, we have performed  $r^{-6}$  ensemble averaging of the intermolecular distance restraints during the structure calculation (Chapter III). Even without the averaging, the restricted motional freedom of the attached MTSL cannot account for the large violations observed. For example, the confined motion of MTSL attached to N200C CcP (Figure 3.8 B, p. 57) could not give rise to the violations as large as 10–15 Å (Figure 4.1 B).

Being reproducible (Chapter III), the ‘additional’ effects responsible for the violations shown in Figure 4.1 suggest that the calculated structure of the Cyt *c* – CcP complex is not sufficient to explain all observed paramagnetic effects. These additional effects could have several causes, such as non-specific interactions caused by random collisions, binding of two Cyt *c* molecules to CcP<sup>109-111,200</sup>, and dynamics within the protein complex. The first two possibilities imply the presence of distinct complexes, in which Cyt *c* is bound with different affinities. If this is the case, lowering Cyt *c* concentration in a sample with a constant concentration of CcP would result in a decrease of the fraction of the weaker complexes. This decrease would lead to a reduction of the contributions from the weaker complexes to the PREs, resulting in fewer violations and a non-uniform concentration-dependence of PREs. Contrary to that, in the case of dynamics within the complex, lowering the Cyt *c* concentration should not influence the contribution of the dynamic encounter state to the PREs. Control experiments with the lowered Cyt *c* concentration and N200C CcP, selected because MTSL attached at this position produces the largest violations (Figure 4.1 B), have shown that the additional paramagnetic effects are independent of the Cyt *c* concentration in the range used (see Results). This finding is in agreement with the concept of a dynamic ensemble of multiple protein orientations within the complex.

***Dynamics within the Cyt *c* – CcP complex***

The dynamics within Cyt *c* – CcP complex is a well-reported phenomenon (ref. 87,120 and references therein). In our case it is evidenced by the additional paramagnetic effects, which could only be adequately explained by a complex comprised of an equilibrium between a well-defined, single-orientation form and a dynamic state (Figure 1.1, p. 11). Due to the sixth-power distance-dependence of the paramagnetic relaxation, a dynamic state will contribute to the PREs for the residues that get close to MTSL, even if this state is populated for only a few percent of the time. Thus, the observed paramagnetic effect represents a sum of PRE contributions from all protein – protein orientations within the complex (Equation 4.1 in Materials and Methods), corresponding to the combination of the dominant, well-defined form and multiple conformations of the complex sampled in the dynamic encounter state.

We have estimated that Cyt *c* and CcP spend > 70 % of the lifetime of the complex in the dominant, well-defined form that is observed in the solution structure (Figure 3.10, p. 63). This finding is consistent with other studies that have proposed the existence of a single-orientation complex in solution<sup>127-129</sup>. In particular, large NMR chemical shift perturbations of Cyt *c* resonances upon complex formation suggest the presence of a dominant protein – protein orientation<sup>129</sup>, as for more dynamic protein complexes the perturbations tend to be smaller (ref. 11,12,146,201 and Chapter V). Our conclusions contrast sharply with the findings of an earlier NMR study that proposed the existence of a highly-dynamic Cyt *c* – CcP complex in solution, with the proteins spending only a small fraction of time, if any, in the well-defined, structurally-specific form<sup>123</sup>.

Semi-quantitative analysis of the additional paramagnetic effects have allowed us to define the conformational space occupied by the proteins in the dynamic encounter complex (Figure 4.2 A). In the dynamic state, the binding interface on CcP is localized around the Cyt *c* position in the dominant orientation. This finding is in agreement with the view that an encounter complex facilitates formation of the dominant one via pre-orientation of the protein molecules and reduced-dimensionality search<sup>18,120</sup>. The CcP binding surface contains a part of the negatively-charged region predicted to interact with Cyt *c* by a classical Brownian dynamics study<sup>26</sup>, suggesting that electrostatic attraction

plays a dominant role in determining the nature of the encounter complex. Clearly, the binding interface on CcP is larger than that observed in the crystal<sup>107</sup> or solution structure (Chapter III), with an earlier NMR chemical shift perturbation analysis showing the same to be true for Cyt *c*<sup>129</sup>. Several reports described CcP binding effects on the rear of Cyt *c* in solution<sup>123-125,129</sup>, and a recent study of complexes between CcP and different variants of Cyt *c* has reported crystal structures in which Cyt *c* is positioned with its back towards CcP<sup>198</sup>. If employed in the dynamic state of the complex, such binding modes would explain the paramagnetic effects at the back of Cyt *c* (Figure 4.1 A).

By defining the conformational space of an ensemble of protein orientations (this Chapter) and characterizing the dominant structure of the complex (Chapter III), we were able to address both sides of the equilibrium of the complex formation between Cyt *c* and CcP in solution. We show that the dominant orientation of the protein complex is in equilibrium with a dynamic state that contributes to the observed intermolecular effects. Semi-quantitative analysis of the additional paramagnetic effects allows us to define the conformational space occupied by the protein molecules in the dynamic state. The present experimental approach provides a unique focus on the role of dynamics in biomolecular interactions that will be useful for study of other biological macromolecular complexes in solution.

## ***Materials and Methods***

A detailed description of the protein and NMR sample preparation, NMR experiments, determination of intermolecular PREs and their conversion into distance restraints, and the structure calculations of the Cyt *c* – CcP complex is given in Materials and Methods of the Chapter III.

NMR samples of the control experiment described in this Chapter contained 0.3 mM CcP-MTS or CcP-MTSL and 0.06 mM <sup>15</sup>N Cyt *c* in 20 mM NaP<sub>i</sub> 0.1 M NaCl pH 6.0, 6 % D<sub>2</sub>O for lock, and 0.1 mM CH<sub>3</sub>CO<sup>15</sup>NH<sub>2</sub> as an internal reference. The pH of the samples was adjusted to 6.00 ± 0.05 with small aliquots of 0.1 M HCl or 0.1 M NaOH. Measurements were performed at 301 K on a Bruker DMX600 spectrometer equipped with a triple-resonance TCI-Z-GRAD CryoProbe (Bruker, Karlsruhe, Germany). 2D [<sup>15</sup>N, <sup>1</sup>H]

HSQC spectra were acquired with 2048 and 512 complex points in the direct and indirect dimensions, respectively, and spectral widths of 32 ppm ( $^{15}\text{N}$ ) and 16 ppm ( $^1\text{H}$ ) and analysed as described in Materials and Methods of the Chapter III.

### ***Conformational space of the encounter complex***

For each Cyt  $c$  residue, the observed paramagnetic effect ( $R_{2,obs}^{para}$ ) represents a sum of PRE contributions ( $R_2^{para}$ ) from  $n$  protein orientations within the complex, weighted by the fraction of time ( $f$ ) spent in each of them, Equation 4.1:

$$R_{2,obs}^{para} = \sum_{i=1}^n f_i R_{2,i}^{para} \quad (4.1)$$

In order to delineate the conformational space explored by Cyt  $c$  in the complex with CcP as shown in Figure 4.2 A, the largest distance between a backbone nucleus of Cyt  $c$  and MTSL that would result in a significant ( $\geq 7$  Hz)  $R_{2,obs}^{para}$  with  $f = 0.03$  was calculated to be 12 Å. Thus, the nuclei that experience additional PREs (Figure 4.1) must spend *at least* 3% of the time at this distance from MTSL or less time at a shorter distance. Cyt  $c$  nuclei spend *at most* 3% of the time at 12 Å from those spin-labels that exert no paramagnetic effects and even less time at shorter distances. Use of a somewhat arbitrary value of  $f = 0.03$  is justified as, due to  $r^{-6}$  dependence, very similar results are obtained for other  $f$  values as can be appreciated from Figure 4.2 B and C.

To define the space that must be occupied or is avoided by the centre of mass of Cyt  $c$  (Figure 4.2 A), red and blue spheres, respectively, were constructed around the oxygen atom of MTSL with the radius of 12 Å plus the average distance from the Cyt  $c$  centre of mass to its surface (14 Å). Only the segments of the red and blue spheres that are between 12 and 19 Å from the surface of CcP are retained. The former corresponds to the closest approach of the centre of mass of Cyt  $c$  to the surface of CcP, while the latter denotes the furthest distance from CcP at which the proteins still form a complex. In case of an overlap, blue space is given priority over red. The segments around MTSL attached at N38C, N200C, and T288C are in red, while those around T137C and S263 are in blue.